American Mineralogist, Volume 69, pages 1015–1024, 1984

An experimental investigation of the chlorite terminal equilibrium in pelitic rocks

JAMES R. BURNELL, JR.[1] AND MALCOLM J. RUTHERFORD

Department of Geological Sciences, Brown University
Providence, Rhode Island 02912

Abstract

Experiments on the stability of chlorite in the presence of muscovite and quartz were performed in the system K_2O–MgO–FeO–Al_2O_3–SiO_2–H_2O. The hydrothermal experiments were done at the quartz–fayalite–magnetite oxygen buffer using both natural and synthetic crystalline starting materials. Results of the experiments show that chlorite of intermediate Fe/Mg is stable to higher temperatures (at a given pressure) than the end-member compositions. Chlorite is more magnesian than co-existing biotite but plots to the Fe-side of the tie-line connecting coexisting biotite and cordierite on the AFM diagram.

Magnesian chlorite breaks down in metapelitic rocks by the continuous reaction

chlorite + muscovite = biotite + cordierite + H_2O.

The assemblage chlorite + biotite + cordierite + muscovite + quartz exists stably over a narrow temperature range at a given pressure and for a very small range of rock composition.

The terminal reaction involving an Al_2SiO_5 phase, by which chlorite disappears is

chlorite + muscovite = cordierite + biotite + Al_2SiO_5 + H_2O.

The reversed experiments have constrained the univariant assemblage chlorite–cordierite–biotite–Al_2SiO_5 as lying between the points 640±10°C at 4 kbar and 612±12°C at 2 kbar. This implies that chlorite (of intermediate Fe/Mg) is stable to higher temperatures in metapelites than has been hypothesized, and chlorite can coexist stably with sillimanite according to the Al_2SiO_5 triple point of Holdaway (1971).

Introduction

A major goal of the metamorphic petrologist is to determine as closely as possible the pressure, temperature and activities of mobile components at the peak of metamorphism. To this end, pelitic rocks have proven valuable due to their sensitivity to changes in pressure–temperature conditions and the utility of viewing the assemblages in AFM projection (Thompson, 1957). The *P–T* topologies of univariant reactions in pelitic rocks have been calculated by numerous workers (e.g., Albee, 1965; Hess, 1969; Hoschek, 1969; Grant, 1973; A. B. Thompson, 1976b; Dickenson, 1981). These "petrogenetic grids" provide a basis from which to view the general relationships of mineral assemblages and provide a qualitative starting point for interpretation of naturally-occurring assemblages. It remains for the experimentalist to quantify the conditions at which various reactions occur and thus to accurately position the grids in P_{H_2O}–T–f_{O_2} space.

This paper reports on an experimental investigation of the terminal equilibrium of chlorite and the continuous reaction by which chlorite breaks down to form biotite and cordierite. In the system K_2O–Al_2O_3–FeO–MgO–SiO_2–H_2O, there has been some question concerning the proper position of stable chlorite in AFM projection. Albee (1965) and Harte (1975), theorized that chlorite lies to the Mg-side of the biotite–cordierite tie-line. If this is the case in nature, the range of stable chlorite compositions will shrink to the Mg-side of the AFM diagram with increasing grade, and Mg-chlorite will disappear by terminal reaction to the assemblage Mg-cordierite + Mg-biotite (Fig. 2). Based on data from natural assemblages, Hess (1969) predicted that chlorite lies on the Fe-side of the biotite–cordierite tie-line, a view supported by Tewhey and Hess (1975), Guidotti et al. (1975) and Ryerson (1978). If this is true, chlorite is an interior phase in AFM projection (interior to the apices Bt–Crd–Al_2SiO_5) and must disappear by terminal reaction *within* the AFM volume, i.e., the chlorite stable to the highest grades would be of intermediate Fe/Mg ratio (Fig. 3). A study of the terminal equilibrium of chlorite is important in determining which of the two predicted AFM topologies is

[1] Present address: Basalt Waste Isolation Project, Rockwell Hanford Operations, P. O. Box 800, Richland, Washington 99352.

0003–004X/84/1112–1015$02.00

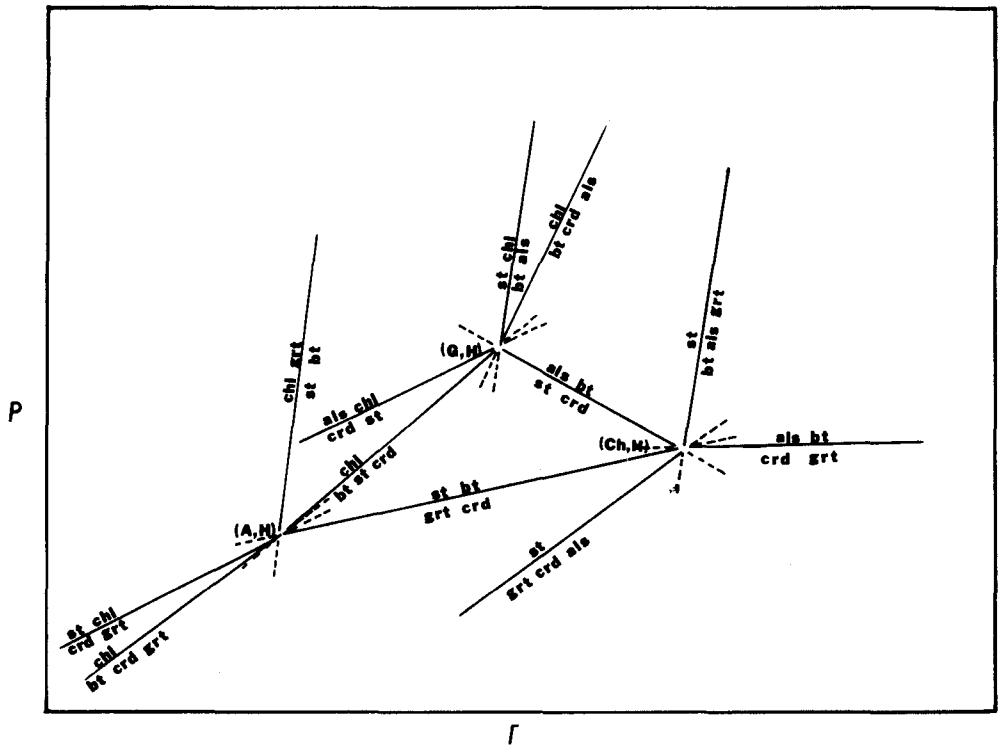

Fig. 1. A schematic *P-T* petrogenetic grid showing the location of the discontinuous reaction

$$Chl + Ms = Crd + Bt + Als$$

(after Hess, 1969). The reaction emanates from the invariant point for reactions which do not involve garnet or hypersthene (G, H). None of the reactions have been located experimentally in the system K_2O–FeO–MgO–Al_2O_3–SiO_2–H_2O and consequently none of the invariant points have been definitively located in *P–T* space.

correct. It should reveal the reactions by which chlorite disappears in prograde metamorphism and at what *P–T* conditions these reactions occur.

The correct placement of the chlorite univariant reaction on the *P–T* grid constrains the location of the invariant point for the group of garnet- or hypersthene-absent univariant reactions ("G,H" of Hess, 1969). The univariant lines representing these five reactions must all intersect at a single point in *P–T* space (see Fig. 1). The determination of the exact position of two appropriate reactions will locate the position of the invariant point and make it possible to better define the grid topology. The experiments should thus allow quantitative estimates of the pressures and temperatures at which natural chlorite-bearing pelitic assemblages were formed.

Portions of this system have been studied experimentally by other investigators. Seifert (1970), Bird and Fawcett (1973), and Chernosky (1974) studied the stability of pure Mg-chlorite; Turnock (1960) and James et al. (1976) investigated pure Fe-chlorite; McOnie et al. (1975) and Fleming and Fawcett (1976) both investigated the Fe–Mg chlorite solid solution in K_2O-free systems. Hirschberg and Winkler (1968) investigated the reaction of interest (Chl = Bt + Crd + Als) using natural chlorites. The data in these papers are valuable constraints on the experiments in the synthetic AFM system.

Experimental methods

Apparatus

The experiments were conducted in standard cold-seal pressure vessels of Rene 41 alloy. Temperatures were monitored with chromel-alumel thermocouples and were checked at least daily. Variations from the mean temperature were usually less than 5°C. Thermocouples have been calibrated against the melting point of NaCl and Zn metal and the run temperature is within ±5°C of the recorded value. Pressure was monitored by a 100,000 psi Astra gauge periodically calibrated against a Heise gauge. It was found that pressure varied by less than 1% over the period of a run and the pressures are considered accurate to within ±1%. The techniques used were standard for hydrothermal experiments with the oxygen fugacity controlled using the solid buffer technique (Eugster and Wones, 1962). The results

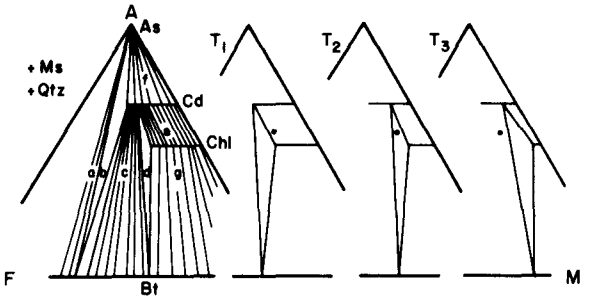

Fig. 2. Graphical representation of behavior of chlorite as an "exterior" phase in AFM projection. A schematic diagram showing the stable Mg-rich mineral assemblages for the facies under discussion. T_1–T_3 show the progressive shift of the 3-phase field cordierite–biotite–chlorite with increasing temperature. The circle represents a rock bulk composition. At the lower temperature, a rock of the specified composition contains cordierite + chlorite (+ muscovite and quartz). As temperature increases to T_3, biotite forms, and the assemblage becomes cordierite + chlorite + biotite (+ muscovite and quartz). As temperature increases to T_4, chlorite disappears from rocks of the designated composition leaving the assemblage cordierite + biotite (+ muscovite and quartz). At high temperatures chlorite occurs only in rocks of very high Mg-content.

reported herein were all done at the quartz–fayalite–magnetite (QFM) buffer.

The nature of the experimental run products was determined by both optical inspection and X-ray diffraction, comparing run products with starting materials in both methods. Fe/Mg ratios of ferromagnesian phases in the run products were determined with an ARL electron microprobe. The powdered material was placed on a pure silica-glass slide and dispersed with several drops of acetone, allowed to dry and then carbon-coated in the conventional manner. A visual search was made to locate identifiable grains of biotite and cordierite and as many grains were probed as possible in a given mount (usually 20–30 grains of each mineral). A working curve was constructed at each probe session using standards of cordierite and biotite of known Fe/(Fe+Mg). The compositions of the unknowns were read directly from the curves. The Fe/(Fe+Mg) values listed are based on the results from 20–30 grains with a maximum spread of ±5 mol % (nearly always ±2–3 mol %).

Natural biotite standards were ground as fine as possible and dispersed on a slide using the same technique as for the synthetic material. It is possible that the biotite plates may have been sufficiently thin to introduce a systematic error into the analysis from each run; specifically, thin plates would tend to yield "apparent" Fe/(Fe+Mg) values, higher than thick plates (Solberg et al., 1981). Because the analytical system allowed the determination of only 3 elements at a time, total analyses were not made and, consequently the effect of this factor was not investigated specifically. Care was taken, however, to consider for analysis only those unknowns for which the count rate was similar to that of the standards. Also, the count rate for biotite products was the same as for cordierite products. (Because cordierites were thick blocky grains, the similarity of count rates between them and the biotites was taken to indicate that the thickness of the biotites was adequate to yield a reliable Fe/Mg ratio).

The analyses were done at conditions of 15 kV accelerating potential 0.1 μA beam current, with a beam diameter of approximately 1 μm.

Mineral phases

Crystalline starting materials were used in all runs. Synthetic phases were crystallized from reagent-grade chemicals prepared in the same manner as described by Richardson (1968).

Quartz: The quartz used was natural material from Lake Toxaway, ground and washed in H_2SO_4.

Andalusite: Andalusite was natural gem-quality material from the teaching collection of Brown University. Microprobe analysis showed that this contains 0.33 wt.% Fe_2O_3 and 0.05 wt.% MnO.

Sillimanite: Sillimanite was natural material from Brandywine Springs, PA (Richardson et al. 1969).

Cordierite: Cordierite was crystallized in Ag capsules from stoichiometric gels prepared in 0.1 increments of Fe/(Fe+Mg). The gels were run for seven days at 700°C and 1.5 kbar at the G-CH_4 buffer. The resulting cordierites were euhedral, rectangular crystals, 25–50 μm in length. More Fe-rich compositions contained small bleb-like inclusions of a green isotropic substance (probably hercynite) and only those syntheses which provided clean cordierite or crystals with a very small amount of the green inclusions were used.

Cordierites formed in run products (from the breakdown of chlorite) were clean and inclusion-free and were generally smaller (15–25 μm) than those crystals formed in the syntheses.

Biotite: Synthetic biotites were prepared in the same manner as the cordierites except that the temperature of the synthesis was 500°C. The compositions used were along the siderophyllite-eastonite join, $K_2(Mg,Fe)_5Al_3Si_5O_{10}(OH)_2$. The synthetic biotites consisted of clumps of extremely fine crystals identified by X-ray diffraction. No phases other than biotite were identified optically.

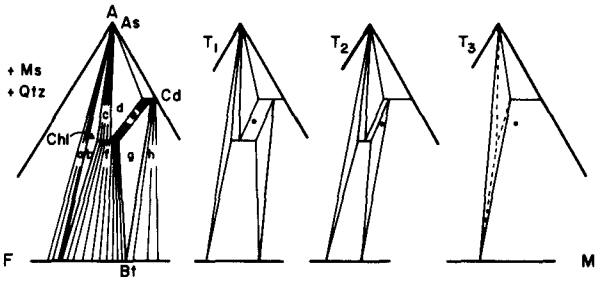

Fig. 3. Schemiatic AFM representation of chlorite as an interior phase showing the assemblages present. The bulk composition noted consists of the 2-phase Crd–Chl assemblage at low temperatures (T_1). As T increases, the field g (Chl–Crd–Bt) migrates away from the Mg-sideline eventually crossing over the bulk composition at which point biotite is formed, and the rock now consists of the assemblage Bt–Crd–Chl (T_2). Note that the range of stable chlorite compositions is also shrinking from the Fe-side of the diagram as the continuous reaction Chl + Ms = Bt + Als consumes Fe-rich Chl with increasing T (migration of field toward center of diagram). At T_3 the range of chlorite compositions stable at lower temperatures has shrunk to a single composition.

Biotites produced by the breakdown of chlorite were much larger, appearing as thin hexagonal plates which varied in size from 5–20 μm in diameter.

Chlorite: Chlorites were synthesized from stoichiometric oxide mixes of composition $[(Fe,Mg)_7Al_2][Al_2Si_4]O_{15}(OH)_{12}$ with Fe/(Fe+Mg) of 0.1, 0.3, 0.45, 0.5, 0.6, and 0.7. The oxide mixes were sealed with water in Ag capsules and run at 500°C and 5.5 kbar for seven days. The f_{O_2} during the synthesis runs was fixed at that of QFM or Ni–NiO buffer. The synthetic chlorites consisted of felty masses of extremely fine green plates. The mineral was identified by its typical thuringite X-ray diffraction pattern (ASTM card 7–78). The presence or absence of chlorite in runs was monitored using the (001) peak; the other peaks were interfered with by various run products.

Muscovite: Muscovite was synthesized from a stoichiometric oxide mix at 500°C and 2 kbar for three days. As with the other phyllosilicates, the synthetic muscovite consisted of aggregates of extremely small crystals and was identified by X-ray diffraction.

Run procedures

The experimental runs were designed to determine the range of stable chlorite compositions in terms of Fe/(Fe+Mg) at a given *P–T*. To test the stability range of chlorite, charges were prepared of the following materials: chlorite of known Fe/(Fe+Mg), seeds of cordierite of the same Fe/(Fe+Mg), quartz, muscovite in excess of chlorite, and seeds of Al_2SiO_5. In this manner, the bulk composition was constrained to lie along a line from the aluminosilicate apex of the AFM diagram through the Fe/(Fe+Mg) ratio of interest. Seeds of cordierite and Al_2SiO_5 were used for two reasons. Primarily, this enhances the growth of these phases, which experience showed do not nucleate readily in unseeded runs. Also, the use of small amounts served to remove the AFM bulk composition of the system from the chlorite single-phase field while keeping it near the "wide" part of the 3-phase Bt–Crd–Chl field (see Fig. 3).

Starting materials containing biotite and/or cordierite instead of chlorite were used to reverse the reaction by causing the growth of chlorite.

All charges were run at temperatures of 575, 600, 625, 640 and 650°C and at 2, 3, and 4 kbar P_{H_2O}. Reversals were obtained in several cases to provide brackets on the univariant reaction in *P–T* space. These were accomplished by using run products in which chlorite had completely reacted away and running the experiment at lower temperatures to achieve chlorite growth.

Experimental results

The Chl–Crd–Bt continuous reaction

The range of stable chlorite compositions for each set of external variables was tested by running a series of experiments in which *P*, *T*, and f_{O2} were constant and the Fe/(Fe+Mg) of the starting materials was varied. The presence or absence of chlorite was as an indicator of the correct topology.

Table 1 contains the results of the experiments indicating that, for a given pressure, chlorite of intermediate Fe/(Fe+Mg) persists to higher temperature than the more magnesian (and ferroan) end-members. In runs with starting materials to the Mg-side of the stable chlorite range, chlorite was lost in favor of the Bt–Crd–(Ms–Qtz) assemblage, indicating that the "chlorite interior" topology is the correct representation. Combining the stability data with analyzed compositions of biotite, and cordierite which coexist with chlorite, *T–X* loops can be constructed to show the compositional variation of the three ferromagnesian phases involved in the continuous reaction. (A good treatment of the use of *T–X* loops in describing continuous metamorphic reactions is found in A. B. Thompson, 1976a). These data are presented in Figure 4 for the reaction at 2, 3, and 4 kbar. The loops were constructed to conform with the results of the runs from Table 1, including the compositional data on Crd and Bt formed as run products. (Chlorite compositions, while constrained to lie within the loop, were not specifically determined). Data for the Fe-free system by Seifert (1970) and Bird and Fawcett (1973) were used to anchor the loops on the Fe-free axis.

The *T–X* loops point out three features of the continuous reaction, Chl = Bt + Crd. (1) The compositions of the three Fe-Mg phases all become more Fe-rich with increasing temperature at a given pressure. (2) The 3-phase field is very narrow. Thus the assemblage Chl–Crd–Bt (–Ms–Qtz) can exist in only a limited compositional range in pelitic rocks. (3) The slope of the loops indicates that the compositions change rapidly with temperature, i.e., a magnesian chlorite starts and completes its breakdown in a small temperature range. (4) As pressure increases, i.e., from 2–4 kbar, stable Bt–Crd–Chl assemblages extend to more and more Fe-rich compositions.

The discontinuous reaction

Based on the petrogenetic grids of Hess (1969) and A. B. Thompson (1976b) there are three stable terminal univariant reactions possible in the "chlorite interior" systems by which chlorite can disappear in pelitic rocks if chloritoid is ignored (see Dickenson, 1981). These are

$$\text{Chl} + \text{Ms} = \text{Grt} + \text{Crd} + \text{Bt} + \text{H}_2\text{O} \quad (1)$$

$$\text{Chl} + \text{Ms} = \text{St} + \text{Crd} + \text{Bt} + \text{H}_2\text{O} \quad (2)$$

$$\text{Chl} + \text{Ms} = \text{Als} + \text{Crd} + \text{Bt} + \text{H}_2\text{O} \quad (3)$$

The calculated positions of the three reactions in *P–T* space are shown in Figure 5. For a particular composition the terminal univariant reaction is a function of the pressure and temperature only (at a given f_{O_2}). Reaction (3) was investigated in this study by seeding an Al_2SiO_5 phase in all runs. Over part of the *P–T* range investigated, this reaction may be metastable with respect to reactions (1) or (2). Because garnet and staurolite will not nucleate unless seeded, it is possible to study the reaction involving aluminosilicate. This does not affect the arguments involving chlorite's "interior" position, as all three of the reactions are "terminal" and require chlorite to be an interior phase.

Table 1. Results of hydrothermal experiments

Run	$(Fe/Fe+Mg)_{Mol}$ starting mtrl	P(kb)	T(°C)	Time (days)	Products	$(Fe/Fe+Mg)_{Mol}$ Products
82a	.10	2	575	21	Crd-Bt(?)-Ms-Qtz	
79a	.10	2	600	21	Bt-Crd-Ms-Qtz	Crd .08, Bt .13
75a	.10	2	625	21	Bt-Crd-Ms-Qtz	Crd .10, Bt .12
85a	.10	2	640	21	Bt-Crd-Ms-Qtz	
66a	.30	2	600	14	Chl-Bt-Crd-Ms-Qtz	Crd .24, Bt .34
80a	.30	2	600	18	*Chl-Bt-Crd-Ms-Qtz	Crd .22, Bt .36
78b	.30	2	600	21	Chl-Bt-Crd-Ms-Qtz	Crd .25, Bt .35
76a	.30	2	625	18	Bt-Crd-Ms-Qtz	Crd .24, Bt .35
77b	.30	2	625	21	Bt-crd-Ms-Qtz	Crd .20, Bt .32
81a	.30	2	575	21	Chl-Crd-Bt-Ms-Qtz	
67b	.50	2	600	14	Chl-Bt(?)-Cd-Als(?)	Crd .33
75b	.50	2	625	21	Bt-Crd-Als-Ms-Qtz	Crd .35
84a	.50	2	640	21	Bt-Crd-Als-Ms-Qtz	
81b	.55	2	575	21	*Chl-Bt-Ms-Qtz	
66b	.60	2	600	14	Chl-Crd-(Als)-Ms-Qtz	Crd .40
80b	.60	2	600	18	*Chl-Crd-Als-Ms-Qtz	Crd .37
76b	.60	2	625	17	Crd-Bt-Als-Ms-Qtz	
83a	.60	2	640	21	Crd-Bt-Als-Ms-Qtz	
92a	.10	3	600	28	Crd-Bt-Ms-Qtz	
56a	.30	3	600	28	Chl-Bt-Crd-Ms-Qtz	
55a	.30	3	625	21	Bt-Crd-Ms-Qtz-As+Chl	
88a	.30	3	640	28	Bt-Crd-Ms-Qtz	
56b	.45	3	600	28	Chl-Crd-Ms-Qtz	
50a	.45	3	625	14	Chl-Bt-Crd-Ms-Qtz	Crd .35, Bt .50
87a	.45	3	640	28	Crd-Bt-Ms-Qtz (Mgt)	
46a	.50	3	575	14	Chl-Bt-Als-Ms-Qtz	
45a	.50	3	600	14	Chl-Crd-Als-Ms-Qtz	
50b	.50	3	625	14	Chl-Bt-Crd-Ms-Qtz	Crd .35, Bt .53
87b	.50	3	640	28	Crd-Bt-Ms-Qtz (Mgt)	
46b	.60	3	575	14	Chl-Crd-Al-Ms-Qtz	
52a	.60	3	600	14	Chl-Crd-Ms-Qtz+Bt	
45b	.60	3	600	14	Chl-Crd-Als-Ms-Qtz	
51b	.60	3	625	14	Bt-Als-Ms-Qtz-Cd(?)	Bt .70
88b	.60	3	640	28	Crd-Bt-Als-Ms-Qtz	
55b	.70	3	625	21	Mgt-Bt-Als-Ms-Qtz	
35a	.10	4	575	14	Chl-Crd-Ms-Qtz	
72a	.10	4	625	30	Crd-Bt-Ms-Qtz	Crd .10, Bt .15
70b	.10	4	640	30	Crd-Bt-Ms-Qtz	Crd .09, Bt .15
53a	.30	4	625	14	Crd-Bt-Ms-Qtz	
69b	.30	4	615	14	Crd-Bt-Ms-Q+Chl	Crd .25, Bt .34
70a	.30	4	640	30	Crd-Bt-Ms-Qtz	Crd .22, Bt .37
44b	.45	4	575	14	Chl-Als-Ms-Qtz	
69a	.45	4	615	14	*Chl-Bt-Ms-Qtz	
49a	.45	4	625	14	Chl-Crd-Bt-Ms-Qtz	Crd .35, Bt .49
61b	.45	4	625	14	Chl-Crd-Bt(?)-Als-Ms-Qtz	
54b	.45	4	640	18	Chl-Crd-Bt-Als-Ms-Qtz	Crd .35, Bt .55
37	.50	4	575	14	Chl-Als-Ms-Qtz	
62b	.50	4	600	14	Chl-Crd-Als(?)-Ms-Atz	Crd .42
49b	.50	4	625	14	Chl-Crd-Bt-Ms-Qtz	
47b	.50	4	625	14	Chl-Crd-Bt-Ms-Qtz	Crd .36, Bt .47
65a	.50	4	625	14	*Chl-Crd-Bt(+Als)	Crd .39, Bt .53
47a	.50	4	625	14	Chl-Crd-Bt-Ms-Qtz	
61a	.50	4	625	14	Chl-Crd-Bt(?)-Als-Ms-Qtz	Crd .32
71a	.50	4	640	28	Crd-Bt-Als-Ms-Qtz	Crd .34, Bt .55
18	.50	4	650	21	Crd-Bt-Als-Ms-Qtz	Crd .45, Bt .60
35b	.60	4	575	14	Chl-Bt-Ms-Qtz	
59a	.60	4	600	14	Chl-Als+Crd-Ms-Qtz	
60a	.60	4	625	14	Chl-Als-Crd-Ms-Qtz	Crd .35
63a	.60	4	640	14	+Mgt-Crd-Bt-Ms-Qtz	Crd .35, Bt .49
43b	.70	4	575	14	Chl-Ms-Qtz	
59b	.70	4	600	14	Chl-Als-Ms-Qtz	
60b	.70	4	625	1	+Mgt-Crd-Bt-Ms-Qtz	
63b	.70	4	640	14	+Mgt-Crd-Bt-Ms-Qtz	

1. The charges consisted of chlorite of known Fe/Fe+Mg, Cd seeds of same Fe/Fe+Mg, Ms is excess of Qtz and seeds of Al_2SiO_5.

2. Experiments marked with an asterisk (*) are reversals. Chlorite grew in an experiment which started with a chlorite-free assemblage produced in an earlier experiment.

The discontinuous reaction (3) has been placed at 640±10°C at 4 kbar, 632±7°C at 3 kbar, and 612±12°C at 2 kbar according to the results obtained in this study (Table 1 and Fig. 4). It will be noted in comparing the data

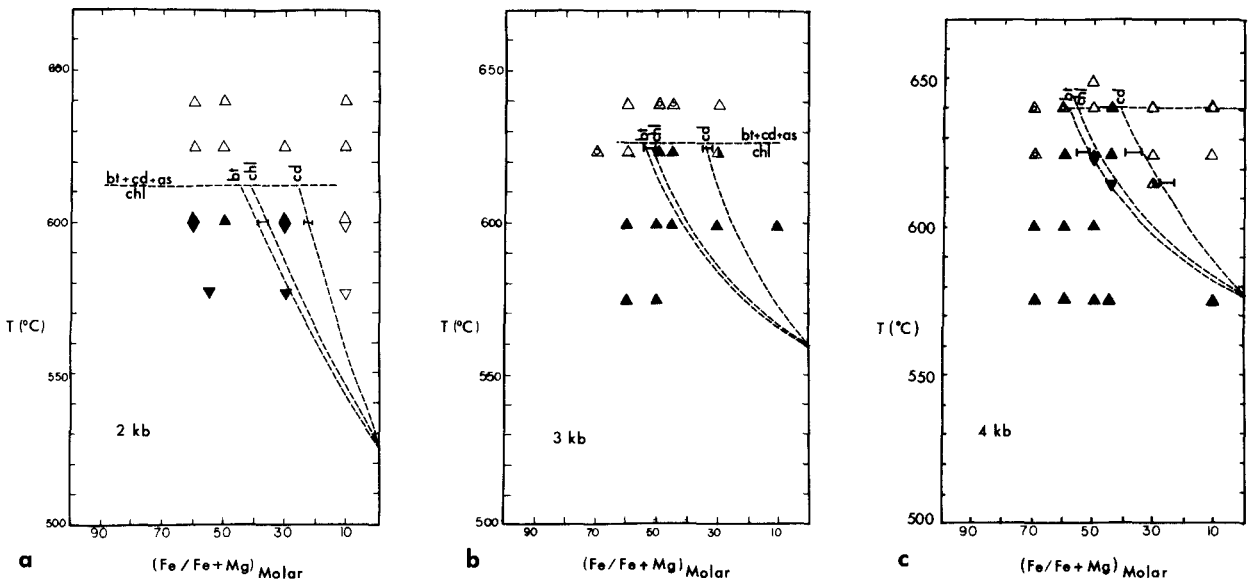

Fig. 4. (a) T–X section for the continuous reaction chlorite + muscovite = biotite + cordierite experimentally determined at 2 kbar. Triangles point the "direction of approach" of each run; those pointing up contained chlorite in the starting materials; those pointing down contained no chlorite in starting material. Open triangles contained no observed chlorite in the run products; solid triangles indicate chlorite was present in the run products. The position of the loops is based on analyzed biotite and/or cordierite compositon (Fe/Mg) in the run products. At a given temperature, the biotite composition is the most Fe-rich, cordierite the most Mg-rich, chlorite intermediate. Error bars indicate range of compositions analyzed. Chlorite compositions in most cases are not based on microprobe analyses but are located schematically. The loop is terminated at high temperature by the reaction chlorite + muscovite = biotite + cordierite + aluminosilicate. (b) T–X loop for the continuous reaction chlorite + muscovite = biotite + cordierite at 3 kbar. Half-filled triangles represent runs in which the presence of chlorite was questionable. Triangles containing circles indicate runs in which magnetite was produced. (c) T–X loop for the continuous reaction at 4 kbar.

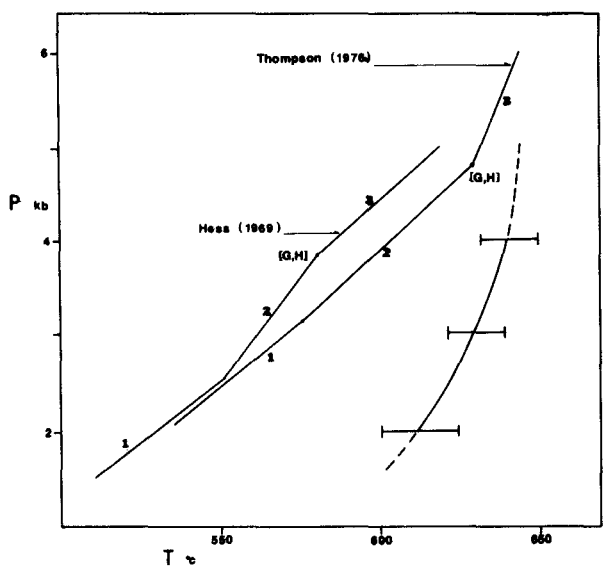

Fig. 5. Locations of reactions 1, 2, 3 in text calculated by Hess (1969) and Thompson (1976b). The curved line is reaction 3 (this study). The invariant point (G, H) must lie on the experimentally-determined line.

in Table 1 with the graphical representation of the T–X loops in Figure 4 that reversals have not been obtained in every possible situation. The reaction has been determined in prograde experiments (increasing temperature resulting in disappearance of chlorite) at 2, 3, and 4 kbar. Reactions have been reversed between 600 and 625°C at 2 kbar, between 625 and 640°C at 3 kbar and between 630 and 650°C at 4 kbar. These data have been combined with the analyzed Fe/(Fe+Mg) compositions of coexisting biotite and cordierite to create the loops. Taken together, these data constrain the location of the loops and the discontinuous reaction.

Discussion

The system K_2O–MgO–FeO–Al_2O_3–SiO_2–H_2O

Experiments on the stability of chlorite have shown that, in the absence of other phases, the Fe-free Mg-chlorite is stable to higher grades than intermediate members of the solid-solution series.

The addition of quartz to the experimental system serves to restrict the stability range of both Fe and Mg-chlorite (Fawcett and Yoder, 1966; James, et al., 1976; Chernosky, 1978). Fleming and Fawcett (1976) reported

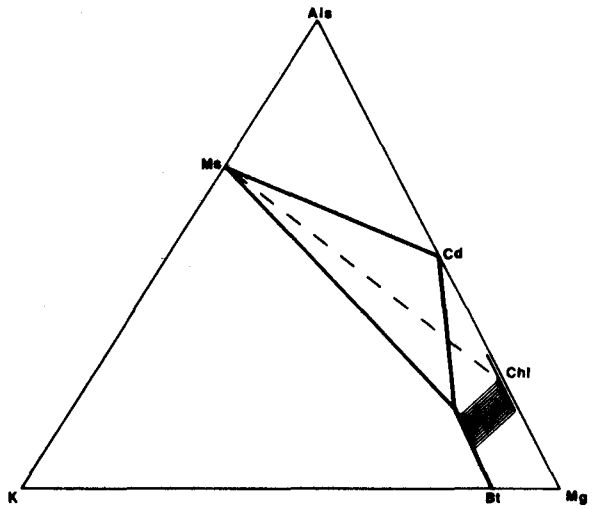

Fig. 6. K–A–M face of K–A–F–M tetrahedron showing the importance of muscovite (Ms) in the experimental system. The reaction by which chlorite disappears in pelitic rocks involves a tie-line switch of muscovite–chlorite = cordierite–biotite. Bulk compositions poor in muscovite would lose muscovite rather than chlorite as a result of the reaction.

that the upper stability limit of chlorite + quartz is virtually independent of Fe/Mg ratio and aluminum content of the chlorite phase.

Experiments in systems without muscovite, however, cannot be directly applied to the equilibrium of chlorite in pelitic rocks. Although its addition to the synthetic system Al_2O_3–FeO–MgO–SiO_2–H_2O introduces complications and increases the difficulty of determining run products, the presence of muscovite is necessary to obtain data relevant to natural pelitic rocks. Figure 6 shows that the break-down of chlorite in the presence of muscovite involves a tie-line switch whereby cordierite-biotite cuts off chlorite from muscovite. In muscovite-poor (or absent) compositions, chlorite can persist to temperatures well beyond its range in pelitic (muscovite-rich) rocks. Thus experimental compositions must lie on the muscovite–chlorite tie-line and contain sufficient muscovite to react with all the chlorite.

Seifert (1970) and Bird and Fawcett (1973) investigated chlorite stability in K_2O-bearing systems and found that the presence of muscovite further restricts the stability range of chlorite. Seifert (1970) found that chlorite + muscovite react to form phlogopite + cordierite at 580 to 590°C at 4 kbar and 525°C at 2 kbar, values we used to anchor our loops on the Fe-free axis.

Nature of the Al_2SiO_5 phase and Al_2SiO_5 reactivity

The experimental work described herein was carried out in a region of *P–T* space in which the identity of the stable Al_2SiO_5 polymorph is unclear because of conflicting data on the position of the triple point (Richardson et al., 1969, Newton, 1966; Holdaway, 1971). With that in mind, andalusite was seeded in most of the runs. Many runs were duplicated using seeds of sillimanite instead, and in no case was there any difference noted in the run products. Because of this the univariant line is treated as continuous within the *P–T* error of the experiments across the andalusite–sillimanite transition.

Because of the notorious non-reactive nature of the aluminosilicate polymorphs, one must also be concerned with the degree of participation of these phases in the reaction. As detailed above, the experiments testing the continuous reaction involved charge compositions between cordierite and biotite on the AFM projection and thus, in most cases, would not contain an Al_2SiO_5 polymorph as a stable member of the product assemblage. Andalusite or sillimanite was included in the starting material of these runs in amounts too small to appear on X-ray diffraction patterns and, consequently, its presence was difficult to monitor by X-ray. In nearly all cases, the aluminosilicate could not be found by visual inspection of the run products, implying that it was reacted *out*.

To test the participation of andalusite in the reaction, two runs (47a and 49a) were spiked with a large amount of andalusite. If andalusite is an active participant in the experimental reactions, the bulk composition of the run system should be shifted to much more aluminous values. The resultant run products should show loss of biotite and growth of cordierite. If andalusite did not participate in the reaction, the effective bulk composition of the charge would remain the same and no change would be seen in the mineralogy of the products. In fact, the runs spiked with andalusite did show a change (runs 61b, 61a, Table 1), most notably the growth of large, abundant cordierite grains. This result indicates that andalusite did, indeed, react in the runs.

Continuous reactions involving Fe-rich chlorite

In the same range of pressure and temperature conditions at which magnesian chlorite is lost by continuous reaction to biotite + cordierite, ferroan chlorite should be consumed in favor of either staurolite + biotite, garnet + biotite, or Al_2SiO_5 + biotite. Because the terminal chlorite reaction involves shrinking the stable compositional range of chlorite from both directions it is important to determine the conditions at which Fe-rich chlorite disappears.

Specific reactions involving garnet and staurolite were not investigated because of the difficulties involved in working with these refractory phases. However, experiments with Fe-rich compositions done in the same manner as the Mg-rich counterparts, yielded self-consistent results and provide constraints on the limits of Fe-rich chlorite + muscovite stability.

Chlorite of Fe/(Fe+Mg) = 0.7 appeared to be stable at 600°C but yielded run products containing magnetite at

625°C at 2 and 4 kbar. Other phases present in the run products were cordierite, biotite, muscovite and quartz. The compositions of cordierite and biotite in this assemblage are essentially the same as those in equilibrium with Al_2SiO_5 under the same conditions: $Fe/(Fe+Mg)_{Crd}$ = 0.35 and $Fe/(Fe+Mg)_{Bt}$ = 0.50. The aluminosilicate-bearing assemblage was produced from a chlorite having an (Fe/(Fe+Mg) = 0.6 (Table 1).

The Mgt–Crd-bearing assemblage produced from the Fe-rich chlorite runs is apparently not the stable one at the *P* and *T* of interest. The stable assemblage, based on the theoretical study of A. B. Thompson (1976a) is staurolite-bearing. Although these products are probably not stable, the appearance of magnetite does indicate that for these conditions the stable chlorite composition is more Mg-rich than the starting composition.

The role of Fe^{3+}

In a discussion of the proper position of chlorite on the AFM diagram, the role of ferric iron must be considered. The Fe/Mg ratio plotted on the AFM diagram should include only Fe^{2+}, as it is this species involved in the Fe–Mg exchange reactions depicted on the diagram. Any Fe^{3+} present will probably occupy lattice sites not directly involved in the migration of tie-lines laterally across the diagram. Traditionally, iron from microprobe analysis is all assigned to Fe^{2+} and used to calculate the Fe/Mg ratio. If some of this is actually Fe^{3+}, there will be less ferrous iron in the mineral than assumed.

Microprobe studies of chlorite–biotite assemblages have shown that the Fe/Mg of these two phases is nearly identical (Chinner, 1960; Mather, 1970; Guidotti et al., 1975; Tewhey, 1975; Ryerson, 1978). If chlorite contains significantly more Fe^{3+} than coexisting biotite, its composition should plot closer to the Mg side of the AFM diagram relative to biotite. This change could theoretically be sufficient to move chlorite to the Mg side of the Bt–Crd tie-line, violating the topological requirements of the "chlorite interior" system. A specific example from biotite zone rocks described by Tewhey (1975), in which the Bt–Crd tie-line falls on the Mg-side of chlorite, requires that chlorite contain 2.3 wt.% more Fe_2O_3 than coexisting biotite to move the tie-line to the Fe-side.

Although this problem can be circumvented by considering the Si/Al ratios of the chlorites, this could not be done with the analytical technique used. The problem was considered, however, and evidence from naturally-occurring phases, synthesized minerals, and from the behavior of the experimental system indicate that Fe^{3+} does not effect the "chlorite interior" topology.

1. Analyses of coexisting biotite and chlorite from Dalradian rocks by Mather (1970) show that, in all his samples, the relative $Fe^{2+}/(Fe^{2+}+Mg)$ of chlorite and biotite changes very little despite widely varying total proportions of $Fe^{3+}/(Fe^{3+}+Fe^{2+})$. In Mather's study, the greatest difference in ferric iron content between chlorite and coexisting biotite was found in a biotite-zone sample. The chlorite contains 28.25 wt.% FeO, 2.91 wt.% Fe_2O_3, the biotite 22.25% FeO, 1.51 wt.% Fe_2O_3. With all iron expressed as Fe^{2+} the molar Fe/(Fe+Mg) of chlorite would be 0.61, biotite 0.63. Subtracting the Fe^{3+}, the molar Fe/(Fe+Mg) for chlorite becomes 0.59 and for biotite 0.62, little different from the original.

2. Samples of synthetic chlorite and biotite used in this study were analyzed by M. P. Dickenson using a refined microtitration technique. The data, for 2 chlorites and a biotite annealed at 550°C on the QFM and NNO buffers, show that chlorite does not contain a significantly greater proportion of Fe_2O_3 than biotite. Within the limits of analytical error the amounts of ferric iron are the same in the two phases.

3. The experimental data showing that the 3-phase Chl–Bt–Crd field sweeps toward more Fe-rich compositions with increasing temperature is itself evidence for the interior position of chlorite. If chlorite plotted to the Mg-side of the Bt–Crd tie-line, the movement of the Chl–Bt-Crd field toward the Fe-side of the AFM diagram would imply that, through prograde metamorphism, a wider and wider range of chlorite compositions would become stable. There is no evidence in natural systems to indicate that this is the case. So it is concluded that Fe^{3+} has no effect on the conclusions drawn from the data.

Applications

As noted above, the fact that the assemblage chlorite–biotite–cordierite exists over only a small range of temperature makes it useful as a geothermometer. According to the present results, rocks which contain this assemblage have been formed in the range of 600–650°C or close thereto. If an independent estimate of pressure is available, this temperature range can be narrowed significantly, likewise, evidence of the discontinuous reaction (3) places the conditions of metamorphism on the univariant line (Fig. 5). However, there are several factors not yet considered which can serve to complicate the situation in natural rocks.

Studies of the mineral equilibria in the thermal aureole of the Cupsuptic pluton, northwestern Maine, by Tewhey (1975) and Ryerson (1978) have shown that the proportion of Mn in the rock can control the presence of chlorite. Ryerson found that in isofacial rocks, which plot identically on the AFM projection, the disappearance of chlorite is a function of the MnO content. Manganese in amounts as little as $Mn/(Mn+Mg)_{Molar}$ = 0.025 in the rock can prevent the appearance of chlorite where it otherwise would occur. When interpreting reactions in rocks, care must be exercised to insure that the presence or absence of chlorite is not simply a function of Mn-content.

As for all dehydration reactions, the equilibrium of the terminal chlorite reaction will be depressed (to lower *T* at a given *P*) if conditions prevailed by which the water pressure was lower than total pressure. Thus the experi-

mental results in this paper represent a maximum stability with regard to temperature.

Conclusions

The results of this experimental study are summarized below. (1) In pelitic rocks containing excess muscovite and quartz, chlorite of intermediate Fe/Mg ratio persists to higher grades than do the Mg and Fe end-members. (2) The continuous reaction by which magnesian chlorite reacts to form biotite and cordierite is a smoothly-varying function of temperature. Magnesian chlorite coexists with biotite and cordierite over such a small range of temperature that the presence of the assemblage in nature is itself a good geothermometer. (3) As predicted by Hess (1969) and A. B. Thompson (1976b) chlorite can disappear by terminal reaction to Als + Bt + Crd. The presence of the 4-phase assemblage Chl–Als–Bt–Crd is univariant (at a given f_{O_2}, $P_{H_2O} = P_T$) in the AFM system and occurs along a line in P–T space which has been constrained between 640±10°C at 4 kbar and 612±12°C at 2 kbar.

The discontinuous reaction (3) originates at the invariant point (G,H) (See Fig. 1) and thus that invariant point must lie somewhere on the univariant line determined for the reaction in this study. Hess (1969) and Thompson (1976b) place (G,H) at 580°C–4 kbar and 625°C–4.75 kbar respectively. The exact position of (G,H) cannot be determined from the results of this study alone, but it is apparent that it lies at somewhat higher temperatures than has been suggested. This may be partly due to the dilution of water by other fluids, which would affect temperatures based on natural occurrences. The effect this has on the petrogenetic grid is to displace other reactions which emanate from (G,H) to higher temperatures also. A more precise positioning of the invariant point in P–T space must await further experimental study.

Acknowledgments

Research was supported by National Science Foundation Grants EAR 75-21894 and 78-13678. Thanks is owed to Paul Hess, Mel Dickenson, Rick Ryerson and Paul Danckworth who provided assistance, advise, and moral support during the experimental work and Eva Lilly and Sheila Arington who typed the many versions of the manuscript. We also thank D. A. Hewitt and J. V. Chernosky for their thoughtful reviews.

References

Albee, Arden L. (1965) A petrogenetic grid for the Fe–Mg silicates of pelitic schists. American Journal of Science, 263, 512–536.

Bird, G. W. and Fawcett, J. J. (1973) Stability relations of Mg-chlorite, muscovite and quartz between 5 and 10 kb water pressure. Journal of Petrology, 14, 415–428.

Chernosky, Joseph V., Jr. (1974) The Upper stability of clinoclore and the free energy of formation of Mg-cordierite. American Mineralogist, 59, 496–507.

Chernosky, Joseph V., Jr. (1978) The stability of clinochlore + quartz at low pressure. American Mineralogist, 63, 73–82.

Chinner, G. A. (1960) Pelitic gneisses with varying ferrous/ferric ratios from Clen Cova, Angus, Scotland. Journal of Petrology, 1, 178–217.

Dickenson, Melville P. (1981) A petrogenetic grid for the KFMASH system. (abstr.) EOS, 62, 421.

Euster, H. P. and Wones, D. R. (1962) Stability relations of the ferruginous biotite, annite. Journal of Petrology, 3, 82–125.

Fawcett, J. J. and Yoder, H. S. (1966) Phase relationships of chlorites in the system MgO–Al_2O_3–SiO_2–H_2O. American Mineralogist, 51, 353–380.

Fleming, Peter D. and Fawcett, J. J. (1976) Upper stability of chlorite + quartz in the system MgO–FeO–Al_2O_3–SiO_2–H_2O at 2 kbar water pressure. American Mineralogist, 61, 1175–1193.

Grant, James A. (1973) Phase equilibria in high-grade metamorphism and partial melting in pelitic rocks. American Journal of Science, 273, 289–317.

Guidotti, C. V., Cheyney, J. T. and Conatore, P. D. (1975) Coexisting cordierite + biotite + chlorite from the Rumford Quadrangle, Maine. Geology, 3, 147–148.

Harte, Ben (1975) Determination of a pelite petrogenetic grid for the Eastern Scottish Dalradian. Carnegie Institution of Washington, Year Book 74, 438–446.

Hess, Paul C. (1969) The metamorphic paragenesis of cordierite in pelitic rocks. Contributions to Mineralogy and Petrology, 24, 191–207.

Hirschberg, A., and Winkler, H. G. F. (1968) Stabilitats bezeichnungen zwischen Chlorit, Cordierit und Almandin bei der Metamorphose. Contributions to Mineralogy and Petrology, 18, 17–42.

Holdaway, M. J. (1971) Stability of andalusite and the aluminum–silicate phase diagram. American Journal of Science, 271, 97–131.

Hoschek, G. (1969) The stability of staurolite and chloritoid and their significance in metamorphism of pelitic rocks. Contributions to Mineralogy and Petrology, 22, 208–232.

James, R. S., Turnock, A. C., and Fawcett, J. J. (1976) The stability and phase relations of iron chlorite below 8.5 kb P_{H_2O}. Contributions of Mineralogy and Petrology, 56, 1–25.

Mather, John David (1970) The biotite isograd and the lower greenschist facies in the Dalradian rocks of Scotland. Journal of Petrology, 11, 253–275.

McOnie, A. W., Fawcett, J. J., and James, R. S. (1975) The stability of intermediate chlorites of the clinochlore–daphnite series at 2 kb P_{H_2O}. American Mineralogist, 60, 1047–1062.

Newton, R. C. (1966) Kyanite–sillimanite equilibrium at 750°C. Science, 151, 1222–1225.

Richardson, Stephen W. (1968) Staurolite stability in a part of the system Fe–Al–SiO–H. Journal of Petrology, 9, 467–488.

Richardson, S. W., Gilbert, M. D. and Bell, P. M. (1969) Experimental determination of kyanite–andalusite and andalusite–sillimanite equilibria, the aluminum–silicate triple point. American Journal of Science, 267, 259–272.

Ryerson, R. J. (1978) Phase Equilibria in the Contact aureole of the Cupsuptic Pluton, Maine. Ph.D. Thesis, Brown University, Providence.

Seifert, F. (1970) Low-temperature compatibility relations of cordierite in haplopelites of the system K_2O–MgO–Al_2O_3–SiO_2–H_2O. Journal of Petrology, 11, 73–99.

Solberg, T., Abrecht, J., and Hewitt, D. A. (1981) Graphical procedures for the refinement of electron microprobe analysis of fine-grained particles. In Roy Geiss, Ed., Microbeam Anal-

ysis, p. 160–162. San Francisco Press, San Francisco, CA.
Tewhey, John (1975) The controls of biotite–cordierite–chlorite–garnet equilibria in the contact aureole of the Cupsuptic pluton, West-Central Maine. Ph.D. Thesis, Brown University, Providence.
Tewhey, John D. and Hess, Paul C. (1975) The controls of biotite–cordierite–chlorite–garnet equilibria in the contact aureole of the Cupsuptic pluton, West-Central Maine. (abstr.) Geological of America Abstracts w/Programs, 7, 1295–1296.
Thompson, Alan B. (1976a) Mineral reaction in pelitic rocks: I. Prediction of P–T–X (Fe–Mg) phase relations. American Journal of Science, 276, 401–424.
Thompson, Alan B. (1976b) II. Calculations of some P–T–X (Fe–Mg) phase relations. American Journal of Science, 276, 425–454.
Thompson, J. B. (1957) The graphical analysis of mineral assemblages in pelitic schists. American Mineralogist, 42, 842–858.
Turnock, A. C. (1960) The stability of iron chlorites. Carnegie Institution of Washington, Yearbook, 59, 98–103.

Manuscript received, May 17, 1983;
accepted for publication, July 16, 1984.